

## OXYGEN ISOTOPE EFFECTS IN MANGANITES: EVIDENCE FOR (BI)POLARONIC CHARGE CARRIERS

Guo-meng Zhao<sup>1,2</sup>, H. Keller<sup>1</sup>, R. L. Greene<sup>2</sup>, and K. A. Müller<sup>1</sup>

<sup>1</sup>Physik-Institut der Universität Zürich,  
CH-8057 Zürich, Switzerland

<sup>2</sup>Center for Superconductivity Research  
Physics Department, University of Maryland  
College Park, MD 20742, USA

### 1 INTRODUCTION

The isotope effects observed in conventional superconductors show that lattice vibrations play an essential role in bringing about superconductivity. In particular, one finds that the superconducting transition temperature  $T_c$  varies as  $T_c \propto 1/M^\alpha$  ( $\alpha \simeq 0.5$ ) when the isotopic mass  $M$  of the material is varied. If lattice vibrations were not important in this phenomenon there is no reason why  $T_c$  should change with the mass of the ions. Thus, the isotope effect provides crucial insight into the microscopic theory of superconductivity in conventional superconductors.

The isotope effects observed in high-temperature superconductors (HTSC) should also place strong constraints on the microscopic pairing mechanism of high-temperature superconductivity. It has been shown that the isotope effects in HTSC are very unusual (see Ref. [1] - [11]). The oxygen isotope shift of the superconducting transition temperature  $T_c$  is small in the optimally doped cuprate superconductors, but the shift is very large, and even much larger than the BCS prediction as the doping is reduced towards the deeply underdoped regime. The large isotope effects in the underdoped cuprate superconductors may suggest that lattice vibrations also play an important role in bringing about high-temperature superconductivity. However the isotope effects cannot be simply explained by the conventional theory of superconductivity. Zhao and coworkers have initiated studies of the oxygen isotope effects on both the penetration depth and the carrier concentration in some cuprate superconductors [6, 5, 4, 8]. The results indicate that the effective supercarrier mass depends strongly on the oxygen isotope mass in the underdoped region, while the carrier concentration is independent of the oxygen isotope mass [6, 4, 8]. These isotope-effect results might suggest that polaronic carriers exist and condense into supercarriers in HTSC, which may give experimental support to the theory of (bi)polaronic superconductivity in HTSC [12].

On the other hand, little attempt had been made to investigate the isotope effects

in magnetic materials before Zhao and coworkers [13] reported an observation of a giant oxygen isotope shift of the ferromagnetic transition in the colossal magnetoresistive manganite  $\text{La}_{0.8}\text{Ca}_{0.2}\text{MnO}_{3+y}$ . This is partly because in most materials, magnetic phenomena at room temperature and below are essentially unaffected by lattice vibrations. The atoms can in general be considered as infinitely heavy and static in theoretical descriptions of magnetic phenomena, so there should be no isotope effects in magnetic materials. However, the magnetic properties in the manganese-based perovskites are beyond what one might expect from the conventional theory of magnetism. The magnetic properties of these materials depend very strongly on the oxygen isotope mass, which suggests that lattice vibrations are important to the basic physics of manganites. In this paper we will begin with a brief review of some theoretical and experimental progress in manganite research in Section 2. We will introduce the concepts of polarons and bipolarons in Section 3. In Section 4, we will continue with a detailed review of various oxygen isotope effects observed in several manganite systems, and their implications for the microscopic mechanisms of the ferromagnetic ordering, charge-ordering and colossal magnetoresistance. The concluding remarks will be given in Section 5.

## 2 EXPERIMENTAL AND THEORETICAL PROGRESS IN MANGANITE RESEARCH

The doped manganites  $\text{Ln}_{1-x}\text{A}_x\text{MnO}_3$  (where Ln is a trivalent rare earth ion and A is a divalent ion) have been found to exhibit some remarkable features. The undoped parent compound  $\text{LaMnO}_3$  (with  $\text{Mn}^{3+}$ ) is an insulating antiferromagnet [14]. When  $\text{Mn}^{4+}$  ions are introduced by substituting a divalent ion (e.g., Ca) for  $\text{La}^{3+}$ , the materials undergo a transition from a high-temperature paramagnetic and insulating state to a ferromagnetic and metallic ground state for  $0.2 \leq x \leq 0.5$  [15]. For  $x \geq 0.5$ , the materials exhibit an insulating, charge-ordered and antiferromagnetic ground state. The temperature at which the insulator-metal transition occurs can be increased by applying a magnetic field. As a result, the electrical resistance of the material can be decreased by a factor of 1000 or more [16, 17], if the temperature is held in the region of the transition. This phenomenon is now known as colossal magnetoresistance (CMR).

The physics of manganites has primarily been described by the double-exchange model [18, 19]. Crystal fields split the Mn 3d orbitals into three localized  $t_{2g}$  orbitals, and two higher energy  $e_g$  orbitals which are strongly hybridized with the oxygen  $p$  orbitals. Each manganese ion has a core spin of  $S = 3/2$ , and a fraction  $(1 - x)$  have extra electrons in the  $e_g$  orbitals with spin parallel to the core spin due to strong Hund's exchange. The electron can hop to an adjacent Mn site with unoccupied  $e_g$  orbitals without loss of spin polarization, but with an energy penalty that varies with the angle between the core spins. This double-exchange model accounts qualitatively for ferromagnetic ordering and carrier mobility that depends on the relative orientation of Mn moments which near  $T_C$  will therefore be strongly dependent on the applied field. However, Millis, Littlewood and Shraiman [20] have pointed out that double-exchange alone cannot fully explain the data of  $\text{La}_{1-x}\text{Sr}_x\text{MnO}_3$ . They suggested that lattice-polaronic effects due to strong electron-phonon coupling (arising from a strong Jahn-Teller effect) should be involved. The basic argument [21] is that in the high-temperature paramagnetic state the electron-phonon coupling constant  $\lambda$  is large and the carriers are polarons, while the growing ferromagnetic order increases the bandwidth and thus decreases  $\lambda$  sufficiently for metallic behavior to occur below the Curie temperature  $T_C$ . The observed giant oxygen isotope effects [13, 22, 23] along with some other experimental results [24, 25, 26] confirm the polaronic nature of charge carriers

in manganites. However, low temperature optical [27], electron-energy-loss (EELS) [28] and photoemission spectroscopies [29] are not consistent with those theoretical models [20, 21, 30]. A broad incoherent spectral feature [27] and a pseudogap in the excitation spectrum [29] were observed while the coherent Drude weight appears to be too small for that of a metal [27]. Recent EELS experiment [28] confirmed the early photoemission and O  $1s$  x-ray absorption spectroscopies [31] of  $\text{La}_{1-x}\text{Sr}_x\text{MnO}_3$ , which showed that the doped holes are mainly of oxygen  $p$  character. However, a substantial mixture between the oxygen  $p$  orbitals and manganese  $e_g$  orbitals has not been ruled out by these experiments. Thus, the present understanding of the physics in manganites is far from complete, and further theoretical and experimental studies are essential.

### 3 POLARONS AND BIPOLARONS

The concept of polarons was first introduced by Landau (1933). If an electron is placed into the conduction band of an ionic crystal, the electron is “trapped by digging its own hole” due to a strong Coulombic interaction of the electron with its surrounding positive ions. The electron together with the lattice distortions induced by itself is called a polaron (lattice polaron). Lattice polarons are not ‘bare’ charge carriers, but are the carriers which are dressed by lattice distortions. Later on, the concept of polarons was treated in much great detail. One of the examples is the Holstein’s treatment where an electron is trapped by self induced deformation of two-atomic molecules (Holstein polaron) [32, 33]. In this case, the polaron moves by thermally activated hopping at high temperatures with a diffusion coefficient  $\omega a^2 \exp[-(E_p/2 - t)/k_B T]$ , where  $a$  is the lattice constant,  $\omega$  is the vibration frequency,  $E_p$  is the polaron binding energy and  $t$  is the bare hopping integral. At low temperatures, the motion of the polarons is coherent, and the polaron behaves like a heavy particle with the effective bandwidth

$$W_{eff} \propto \exp(-\gamma E_p/\hbar\omega), \quad (1)$$

where  $\gamma$  is a dimensionless constant ( $0 \leq \gamma \leq 1$ ) depending on  $E_p/t$ . Höck and coworkers [34] generalized the Holstein model to a system with a strong Jahn-Teller effect. The Jahn-Teller polarons can be formed when the Jahn-Teller stabilization energy  $E_{JT}$  is large compared to the conduction bandwidth. In this case, the polaron binding energy  $E_p$  can be simply replaced by  $E_{JT}$ . Since  $E_p$  is independent of the isotope mass in the harmonic approximation and  $\omega \propto 1/\sqrt{M}$ , Eq. 1 indicates that the effective bandwidth of polarons depends on the mass of ions. In the manganite  $\text{LaMnO}_3$ ,  $E_{JT}$  was estimated to be about 0.5 eV [20] and in  $\text{La}_2\text{CuO}_4$ ,  $E_{JT} \simeq 1.2$  eV (Ref. [35]). Hence one might expect from Eq. 1 that the isotope effect on  $W_{eff}$  should be substantial in both manganites and cuprates.

The concept of a small onsite bipolaron was introduced by Anderson [36], and by Street and Mott [37]. When the attractive interaction between two polarons is larger than the Coulombic repulsion between them, the two polarons can be combined into a real-space pair which is called bipolaron. The onsite bipolaron consists of two polarons sitting on the same unit cell, while the intersite bipolaron includes two polarons sitting on the different unit cells. The onsite bipolaron is very heavy, so a small disorder will make the bipolaron immobile. On the other hand, the effective mass of intersite bipolarons is not so heavy, and thus mobile bipolarons could exist in a real material. The intersite bipolarons were identified in the compound  $\text{Ti}_4\text{O}_7$  (Ref. [38]). At low temperatures, they form a charge-ordered state and are immobile. The recent normal-state susceptibility measurement in the cuprate superconductors  $\text{La}_{2-x}\text{Sr}_x\text{CuO}_4$  [39] indicates that intersite bipolarons coexist with free carriers in the normal-state. The

detailed isotope experiments in this system [8] demonstrate that the mobile intersite bipolarons condense into a superfluid in the deeply underdoped samples.

## 4 VARIOUS OXYGEN ISOTOPE EFFECTS IN MANGANITES

**4.1 Oxygen Isotope Shift of the Curie Temperature.** A first observation of the oxygen isotope effect on the Curie temperature was made in  $\text{La}_{1-x}\text{Sr}_x\text{MnO}_{3+y}$  system by Zhao and Morris (1995) [40]. In Fig. 1, the normalized magnetizations for the  $^{16}\text{O}$  and  $^{18}\text{O}$  samples of  $\text{La}_{0.9}\text{Sr}_{0.1}\text{MnO}_{3+y}$  are plotted as a function of temperature. The oxygen isotope shifts of  $T_C$  were determined from the differences between the midpoint temperatures on the transition curves of the  $^{16}\text{O}$  and  $^{18}\text{O}$  samples. It is clear that the  $^{18}\text{O}$  sample has a lower  $T_C$  than the  $^{16}\text{O}$  sample by  $\sim 6.7$  K. It should be noted that since the value of  $y$  is substantial ( $> 0.05$ ) when samples are prepared below  $1100$  °C, the Curie temperatures in these samples are much higher than that for the corresponding single crystal samples where  $y$  is close to zero [41]. Actually the extra oxygen in the above chemical formula is related to the existence of cation vacancies.

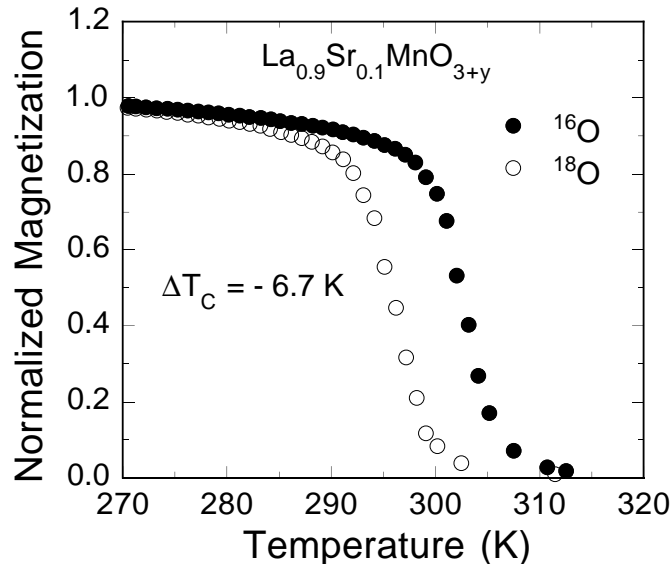


Figure 1: Oxygen isotope effect on the Curie temperature of  $\text{La}_{0.9}\text{Sr}_{0.1}\text{MnO}_{3+y}$ . The figure is reproduced from Ref. [40].

On the other hand, the oxygen-isotope shift of  $T_C$  in  $\text{La}_{0.8}\text{Ca}_{0.2}\text{MnO}_{3+y}$  is very large [13], as seen from Fig. 2. The samples with the same isotope mass have the same  $T_C$ , while the samples with a heavier oxygen isotope mass (about 95% of  $^{18}\text{O}$ ) have a much lower  $T_C$ . The relative isotope shift of  $T_C$  is as large as 10%. Such a large oxygen isotope shift of the ferromagnetic transition is very unusual since lattice vibrations were believed to play no role in the magnetic interactions of most magnetic materials. It is a clear-cut experiment to establish what many have suspected - that atomic motion must be included in any viable description of the manganites [20]. It is also the first experiment in condensed matter physics, which demonstrates that there can be a giant isotope shift of a magnetic transition temperature.

In order to show that the observed isotope effect is intrinsic, we did oxygen isotope back-exchange ( $^{16}\text{O} \rightarrow ^{18}\text{O}$ ;  $^{18}\text{O} \rightarrow ^{16}\text{O}$ ). In Fig. 3, we show the normalized magnetization for the  $^{16}\text{O}$  and  $^{18}\text{O}$  samples of  $\text{La}_{0.8}\text{Ca}_{0.2}\text{MnO}_{3+y}$  before and after isotope back-exchange. The symbol (+) denotes the  $^{16}\text{O}$  sample which has been back-exchanged

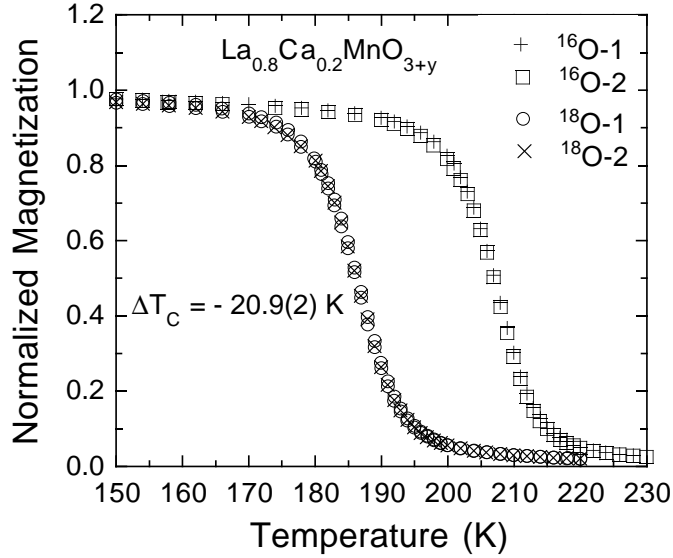


Figure 2: Oxygen isotope effect on the Curie temperature of  $\text{La}_{0.8}\text{Ca}_{0.2}\text{MnO}_{3+y}$ . The figure is reproduced from Ref. [13].

from the original  $^{18}\text{O}$  sample (denoted by open square). The symbol ( $\times$ ) represents the  $^{18}\text{O}$  sample which has been back-exchanged from the original  $^{16}\text{O}$  sample (denoted by open circle). It is evident that the  $T_C$  of the  $^{16}\text{O}$  ( $^{18}\text{O}$ ) sample goes back completely to that of the original  $^{18}\text{O}$  ( $^{16}\text{O}$ ) sample after the isotope back-exchange. This clearly indicates that the shift of  $T_C$  is caused only by changing the oxygen isotope mass.

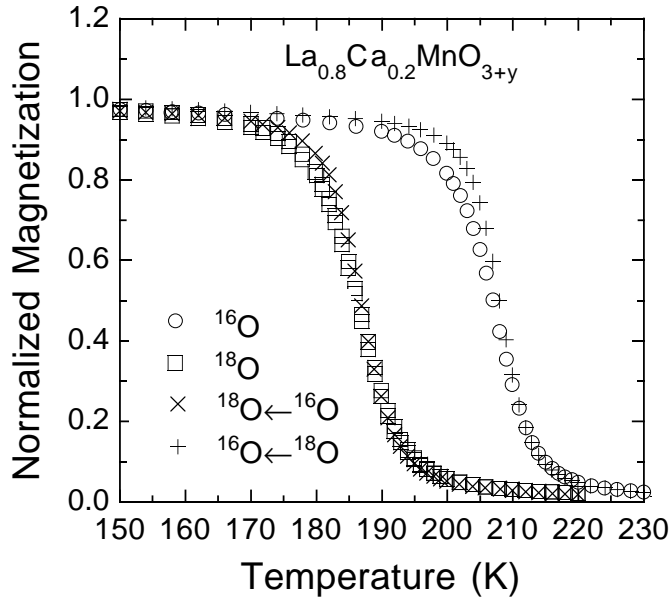


Figure 3: Oxygen isotope back-exchange result for  $\text{La}_{0.8}\text{Ca}_{0.2}\text{MnO}_{3+y}$ . The figure is reproduced from Ref. [13].

The oxygen isotope exponent is defined as  $\alpha_O = -(\Delta T_C/T_C)/(\Delta M_O/M_O)$ , where  $T_C$  and  $M_O$  are for the  $^{16}\text{O}$  sample. With this definition, we obtain  $\alpha_O = 0.85$  for  $\text{La}_{0.8}\text{Ca}_{0.2}\text{MnO}_{3+y}$ , and 0.14 for  $\text{La}_{0.9}\text{Sr}_{0.1}\text{MnO}_{3+y}$ . We have also investigated the oxygen isotope effect on the Curie temperature in other manganite systems. The results are

summarized in Table 1. The magnitudes of  $\alpha_O$  for  $(\text{La}_{0.25}\text{Nd}_{0.75})_{0.7}\text{Ca}_{0.3}\text{MnO}_3$  were

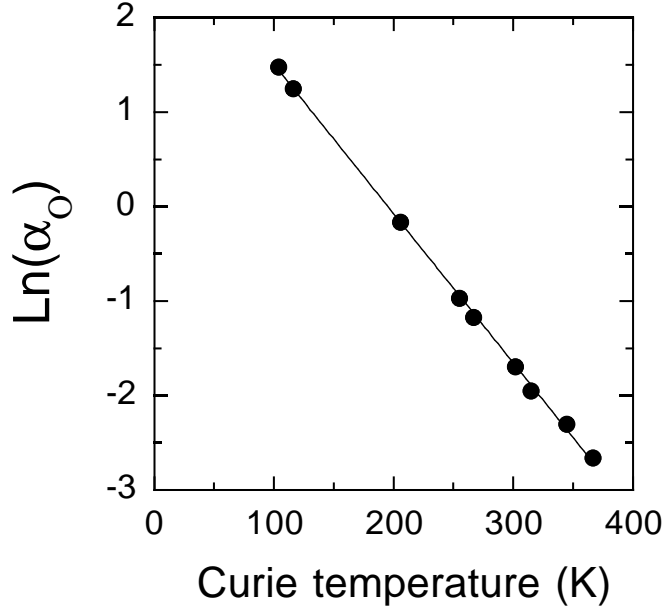


Figure 4:  $\ln(\alpha_O)$  vs the Curie temperatures of the  $^{16}\text{O}$  samples listed in Table 1.

Table 1: Summary of the oxygen isotope effects in manganites

|  | $T_C(^{16}\text{O})$ (K) | $\alpha_O$ |
|--|--------------------------|------------|
| $\text{La}_{0.67}\text{Sr}_{0.33}\text{MnO}_{3+y}$ <sup>a</sup>                                | 367                      | 0.070      |
| $\text{La}_{0.66}\text{Ba}_{0.34}\text{MnO}_{3+y}$ <sup>a</sup>                                | 345                      | 0.10       |
| $\text{La}_{0.85}\text{Sr}_{0.15}\text{MnO}_{3+y}$ <sup>b</sup>                                | 315                      | 0.14       |
| $\text{La}_{0.90}\text{Sr}_{0.10}\text{MnO}_{3+y}$ <sup>b</sup>                                | 302                      | 0.18       |
| $\text{La}_{0.67}\text{Ca}_{0.33}\text{MnO}_{3+y}$ <sup>c</sup>                                | 267                      | 0.31       |
| $(\text{LaMn})_{0.945}\text{O}_3$ <sup>c</sup>   | 255                      | 0.38       |
| $\text{La}_{0.8}\text{Ca}_{0.2}\text{MnO}_{3+y}$ <sup>d</sup>                                  | 206                      | 0.85       |
| $(\text{La}_{0.25}\text{Nd}_{0.75})_{0.7}\text{Ca}_{0.3}\text{MnO}_3$ (warm up) <sup>e</sup>   | 116                      | 3.5        |
| $(\text{La}_{0.25}\text{Nd}_{0.75})_{0.7}\text{Ca}_{0.3}\text{MnO}_3$ (cool down) <sup>e</sup> | 104                      | 4.4        |

<sup>a</sup>Reference [42]

<sup>b</sup>Reference [40]

<sup>c</sup>Reference [22]

<sup>d</sup>Reference [13]

<sup>e</sup>Reference [43]

estimated from both warm-up and cool-down measurements under a pressure of about 10 kbar (Ref. [43]). In Fig. 4, we plot  $\ln(\alpha_O)$  vs the Curie temperatures of the  $^{16}\text{O}$  samples listed in Table 1. It can be seen that all the data points fall on a straight line. So the data can be fit by an equation

$$\alpha_O = 21.9 \exp(-0.016T_C). \quad (2)$$

The above simple empirical relation between  $\alpha_O$  and  $T_C$  is quite unexpected. This relation implies that  $\alpha_O$  has no significant dependence on the concentration of the  $\text{Mn}^{4+}$

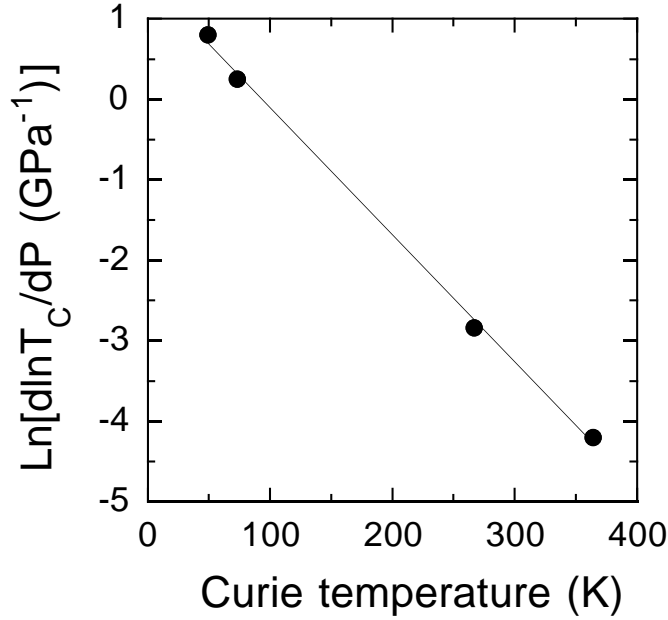


Figure 5:  $\ln(d\ln T_C/dP)$  vs Curie temperature (see text for the data). The quantity  $d\ln T_C/dP$  is the pressure-effect coefficient in the low pressure region.

when it is in the region of 20-35%, as the case of the samples listed in Table 1. From a simple argument based on the double-exchange model and the small polaron theory discussed above, one would expect that  $T_C \propto \exp(-2\alpha_O)$  (Ref. [13]). It is clear that this simple picture cannot quantitatively explain Eq. 2.

In Fig. 5 we show the pressure-effect coefficient  $\ln(d\ln T_C/dP)$  vs  $T_C$  for a fixed  $\text{Mn}^{4+}$  of about 30%. The data are listed as follows:  $d\ln T_C/dP = 2.23 \text{ GPa}^{-1}$  at  $T_C = 49 \text{ K}$  and  $d\ln T_C/dP = 1.29 \text{ GPa}^{-1}$  at  $T_C = 73 \text{ K}$  for  $(\text{La}_{0.25}\text{Nd}_{0.75})_{0.7}\text{Ca}_{0.3}\text{MnO}_3$  (Ref. [44]);  $d\ln T_C/dP = 0.06 \text{ GPa}^{-1}$  at  $T_C = 267 \text{ K}$  for  $\text{La}_{0.67}\text{Ca}_{0.33}\text{MnO}_3$  (Ref. [45]);  $d\ln T_C/dP = 0.015 \text{ GPa}^{-1}$  at  $T_C = 364 \text{ K}$  for  $\text{La}_{0.7}\text{Sr}_{0.3}\text{MnO}_3$  (Ref. [41]). The data can be fit by an equation

$$d\ln T_C/dP = 4.4 \exp(-0.016T_C). \quad (3)$$

Combining Eq. 2 and Eq. 3, one has  $\alpha_O = 5(d\ln T_C/dP)$ . Thus, the isotope exponent is simply proportional to the pressure-effect coefficient. Such a simple correlation between the pressure coefficient and isotope exponent implies that the major effect of the pressure is to increase the phonon frequency. An increase of the phonon frequency by the pressure enhances the ferromagnetic exchange interaction while a decrease of the phonon frequency by increasing the oxygen isotope mass reduces the ferromagnetic exchange interaction. Furthermore, this simple relation between  $\alpha_O$  and  $d\ln T_C/dP$  can be used to check whether the observed oxygen isotope effect is intrinsic. Franck *et al.*, have recently shown that the oxygen isotope exponent in  $\text{La}_{0.8}\text{Ca}_{0.2}\text{MnO}_{3+y}$  is reduced to about 0.4 after the two oxygen-isotope exchanged samples were annealed in argon gas [46]. They considered the isotope effect observed in the argon-annealed samples to be intrinsic. At the same time, they suggested that the giant oxygen isotope shift of  $T_C$  in  $\text{La}_{0.8}\text{Ca}_{0.2}\text{MnO}_{3+y}$  observed by Zhao and coworkers [13] was caused by the existence of extra oxygen in the samples. Their argument is not sound for the following reasons. First of all, the oxygen isotope shift of  $T_C$  is not large in  $\text{La}_{0.9}\text{Sr}_{0.1}\text{MnO}_{3+y}$  where there is substantial extra oxygen (see above), while the oxygen isotope shift of  $T_C$  is colossal ( $>40 \text{ K}$ ) in  $(\text{La}_{0.25}\text{Nd}_{0.75})_{0.7}\text{Ca}_{0.3}\text{MnO}_3$  where there is negligible extra oxygen [43]. Thus the isotope shift has no correlation with the amount of extra oxygen in

the samples. Secondly, there has been no experimental proof that the argon-annealing procedure can ensure the same oxygen contents for the two isotope samples. Actually the argon-annealing is a nonequilibrium procedure, so the reduction rate depends on the diffusion coefficient which is isotope-mass dependent (a heavier isotope mass corresponds to a smaller diffusion coefficient, and thus a slower reduction rate). Only if a thermal equilibrium state is reached during diffusion, can the oxygen contents for the two isotope samples be the same. This has been proved in many previous isotope experiments (e.g., Ref. [4, 6]). Since the pressure effect  $d \ln T_C / dP$  in  $\text{La}_{0.8}\text{Ca}_{0.2}\text{MnO}_{3+y}$  is three times as large as that in  $\text{La}_{0.67}\text{Ca}_{0.33}\text{MnO}_{3+y}$  (Ref. [45]), it is not unreasonable that the observed  $\alpha_O$  ( $\sim 0.85$ ) in  $\text{La}_{0.8}\text{Ca}_{0.2}\text{MnO}_{3+y}$  is about three times as large as that ( $\sim 0.3$ ) in  $\text{La}_{0.67}\text{Ca}_{0.33}\text{MnO}_{3+y}$  (see Table 1).

**4.2 Oxygen Isotope Effect from EPR Measurements.** Electron Paramagnetic Resonance (EPR) is a powerful technique in condensed matter physics, which allows one to study electron-phonon interactions, static and dynamic magnetic correlations on a microscopic level. The temperature dependence of the EPR linewidth includes some

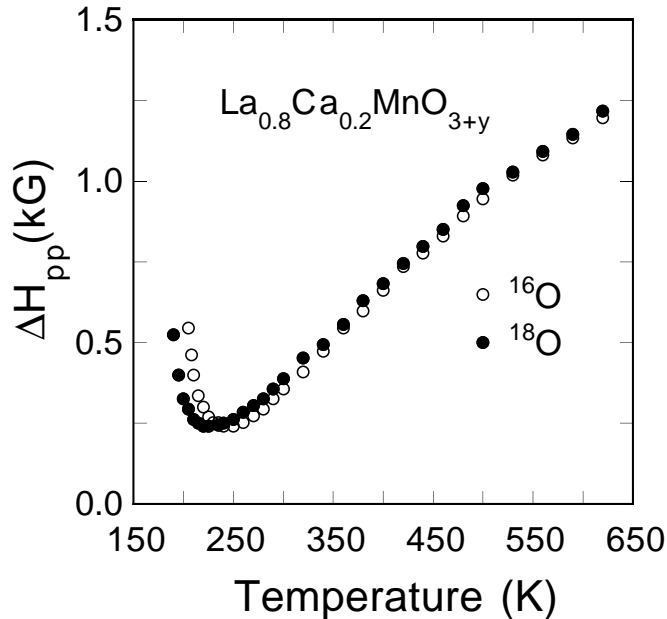


Figure 6: Temperature dependence of the peak-to-peak EPR linewidth  $\Delta H_{pp}$  for  $^{16}\text{O}$  and  $^{18}\text{O}$  samples of  $\text{La}_{0.8}\text{Ca}_{0.2}\text{MnO}_{3+y}$ . The figure is reproduced from Ref. [47].

information about conduction electrons, and the EPR intensity is normally proportional to the static susceptibility. In  $\text{Ti}_4\text{O}_7$  where intersite bipolarons were identified, the EPR intensity follows a Curie-Weiss law as expected, while the EPR linewidth is thermally activated with an activation energy of about 0.08 eV (Ref. [38]). The temperature-dependent part of the linewidth may be directly related to a Korringa-type relaxation of the center through the single polarons whose density is thermally activated.

We performed EPR measurements [47] on the oxygen isotope exchanged samples of  $\text{La}_{0.8}\text{Ca}_{0.2}\text{MnO}_{3+y}$ . The EPR linewidth for the two isotope samples is significantly different below a temperature  $T_{min}$  where the EPR linewidth has a local minimum (see Fig. 6). Since the isotope shift of  $T_{min}$  is similar to the isotope shift of  $T_C$ , the sharp upturn of the EPR linewidth below  $T_{min}$  might be related to the formation of short-range ferromagnetically-ordered clusters. Well above  $T_{min}$ , the EPR linewidths for the two isotope samples have a small difference.

If one assumes that bipolaronic charge carriers also exist in this material, one might expect that the temperature-dependent part of the EPR linewidth should be thermally activated as in the case of  $\text{Ti}_4\text{O}_7$ . It has been shown that [48] the temperature independent part of the EPR linewidth is given by  $\Delta H_o = (\Delta H_{dip})^2 / H_{ex}$ , where  $\Delta H_{dip}$  is the full dipolar width ( $\sim 10^4$  G),  $H_{ex}$  is the exchange field which is proportional to  $T_C$  ( $H_{ex} \sim T_C \sim 10^6$  G). This relation implies that the temperature-independent linewidth of the  $^{18}\text{O}$  sample should be 10% larger than the  $^{16}\text{O}$  sample (since  $T_C$  of the  $^{18}\text{O}$  sample is 10% lower than the  $^{16}\text{O}$  sample). The absolute value of  $\Delta H_o$  should be of the order of 100 G (Ref. [48]). In Fig. 7, we plot the temperature dependence of the EPR linewidth above 300 K. Below 300 K, the ferromagnetic clusters start to form as discussed below. The solid lines in the figure are the best fit curves to the data. The equation used for fitting is given by  $\Delta H_{pp} = \Delta H_o + AT^{-1.2} \exp(-E_a/T)$ . The fit parameters for the  $^{16}\text{O}$  sample are  $\Delta H_o = 84(15)$  G,  $A = 2.11(4) \times 10^7$  GK $^{1.2}$ , and  $E_a = 0.114(15)$  eV. The fit parameters for the  $^{18}\text{O}$  sample are  $\Delta H_o = 129(23)$  G,  $A = 2.11(7) \times 10^7$  GK $^{1.2}$ , and  $E_a = 0.116(26)$  eV. The value of  $\Delta H_o$  for the  $^{18}\text{O}$  sample seems to be larger than for the

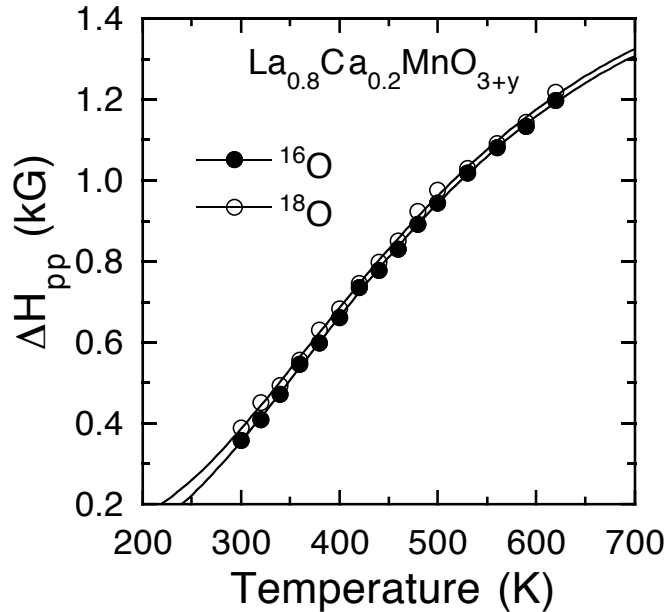


Figure 7: Temperature dependence of the EPR linewidth above 300 K for  $\text{La}_{0.8}\text{Ca}_{0.2}\text{MnO}_{3+y}$ . The data can be fit by  $\Delta H_{pp} = \Delta H_o + AT^{-1.2} \exp(-E_a/T)$ . The data are taken from Ref. [47].

$^{16}\text{O}$  sample, as expected. The parameters  $A$  and  $E_a$  are the same for the two isotope samples within the experimental uncertainty. It is important to note that the activation energy  $E_a$  deduced here is nearly the same as the value (0.121 eV) deduced from the resistivity data of a thin film of  $\text{La}_{0.8}\text{Ca}_{0.2}\text{MnO}_{3+y}$  (Ref. [49]), and that the value of  $E_a$  is nearly equal to the energy gap (0.108 eV) measured from tunneling experiments [49]. These results lead us to suggest that bipolaronic charge carriers should also exist in manganites as in the case of  $\text{Ti}_4\text{O}_7$  (Ref. [38]). Since the bipolarons are heavy and nearly immobile, they have a negligible contribution to the double-exchange. Therefore, the antiferromagnetic superexchange interaction is dominant in the regions where the bipolaronic charge carriers reside, while the ferromagnetic double-exchange interaction dominates in the regions where the mobile polarons sit. The singlet bipolaronic state is not stable with respect to both external magnetic field and ferromagnetic ordering in analogy to the pair-breaking effect in superconductors. Then the density of polaronic carriers increases when an external magnetic field is applied and/or a ferromagnetic

ordering takes place. This picture can naturally explain the CMR effect as well as the metal-insulator transition near  $T_C$ .

In Fig. 8a we plot the inverse EPR intensity  $1/I$  vs temperature. It is clear that the EPR intensity depends strongly on the oxygen isotope mass. Although the unusual

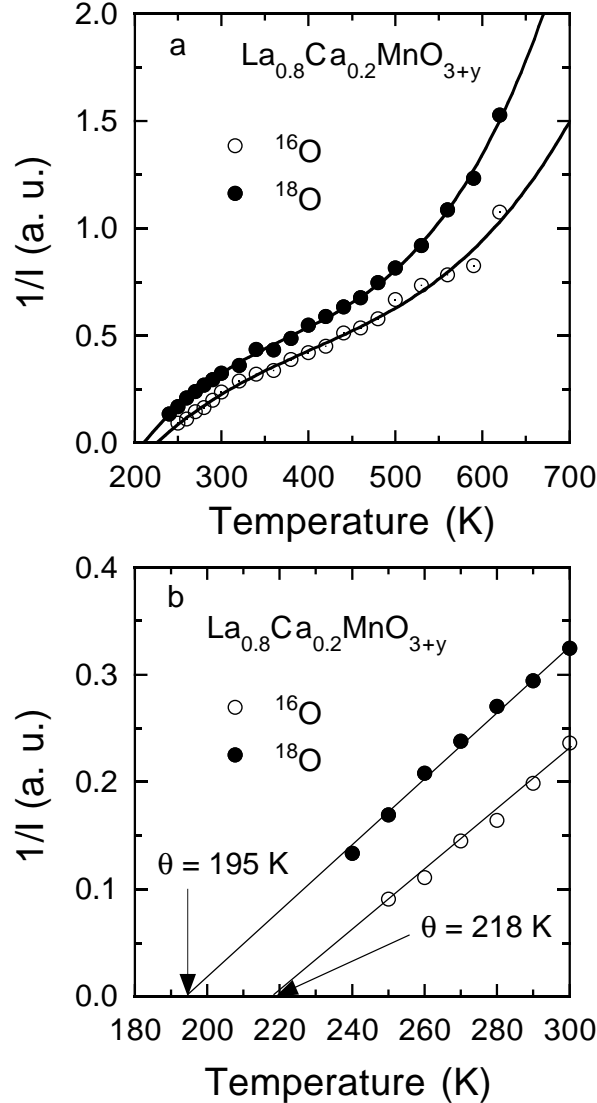


Figure 8: Temperature dependence of the inverse integral intensity of EPR signal for  $^{16}\text{O}$  and  $^{18}\text{O}$  samples of  $\text{La}_{0.8}\text{Ca}_{0.2}\text{MnO}_{3+y}$ . The data are taken from Ref. [47].

temperature dependence of the EPR intensity and its dependence on the oxygen isotope mass could be explained by the so called “bottleneck” effect [47], a conventional interpretation (i.e.,  $I$  is proportional to the static susceptibility) may be more relevant. In Fig. 8b we show  $1/I$  below 300 K. The data can be fit by  $I \propto 1/(T - \theta)$  with  $\theta = 218$  K for the  $^{16}\text{O}$  sample and 195 K for the  $^{18}\text{O}$  sample. For both isotope samples, the  $\theta$  value is almost the same as the  $T_C$  value, which justifies the conventional explanation. Above 300 K, the  $\theta$  value appears to increase with increasing temperature. This is quite reasonable since the density of the mobile polaronic carriers (which are responsible for double-exchange) should generally increase with increasing temperature. On the other hand, a formation of ferromagnetic clusters near  $T_C$  tends to increase the density of the polaronic carriers (since the ferromagnetic ordering can destabilize the bipolaronic state as discussed above). These competing effects might keep the density of the polaronic carriers nearly unchanged at temperatures from 300 K to  $T_C$ . This may explain why

the  $\theta$  value is nearly a constant below 300 K.

**4.3 Oxygen Isotope Effect on the Thermal-Expansion Coefficient.** We have also carried out thermal-expansion measurements [22] on the oxygen-isotope substituted manganites  $(\text{La}_{1-x}\text{Ca}_x)_{1-y}\text{Mn}_{1-y}\text{O}_3$  with a  $\text{Mn}^{4+}$  concentration of  $\sim 33\%$ . The linear thermal-expansion coefficient  $\beta(T)$  exhibits an asymmetric peak at the Curie temperature  $T_C$  and depends strongly on the oxygen isotope mass as shown in Fig. 9. For  $(\text{LaMn})_{0.945}\text{O}_3$  (see Fig. 9a), the  $^{18}\text{O}$  sample has lower  $T_C$  than the  $^{16}\text{O}$  sample by  $\sim 12$  K while the thermal-expansion coefficient jump  $\Delta\beta(T_C)$  of the  $^{18}\text{O}$  sample is larger than that of the  $^{16}\text{O}$  sample by 24(3)%. For  $\text{La}_{0.67}\text{Ca}_{0.33}\text{MnO}_3$  (see Fig. 9b), the oxygen

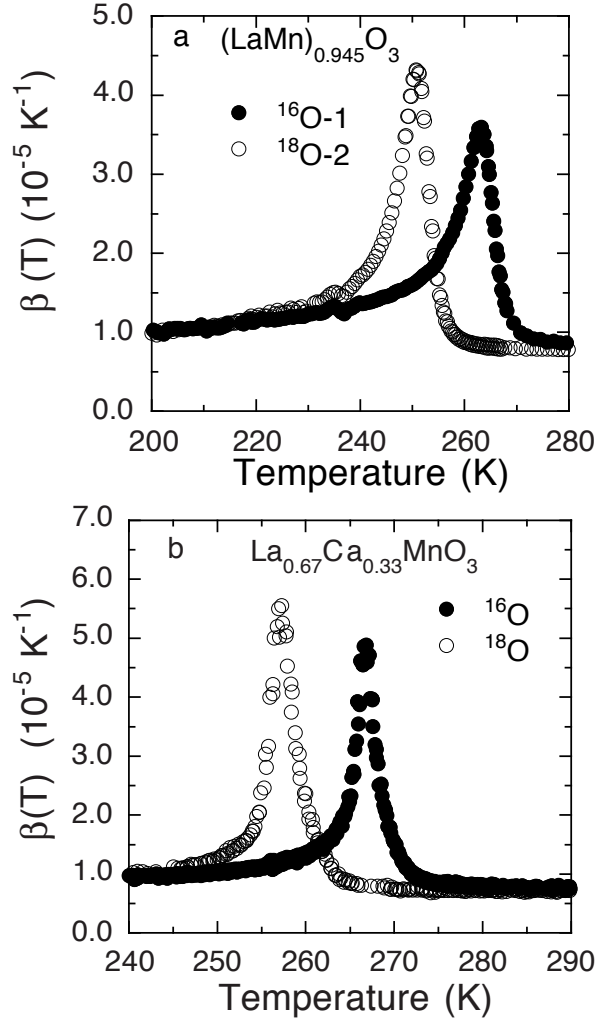


Figure 9: The linear thermal-expansion coefficient  $\beta(T)$  for the  $^{16}\text{O}$  and  $^{18}\text{O}$  samples of  $(\text{LaMn})_{0.945}\text{O}_3$  (a) and  $\text{La}_{0.67}\text{Ca}_{0.33}\text{MnO}_3$  (b). The figure is after Ref. [22].

isotope shift of  $T_C$  is about 10 K while the thermal-expansion coefficient jump  $\Delta\beta(T_C)$  of the  $^{18}\text{O}$  sample is larger than that of the  $^{16}\text{O}$  sample by 16(3)%. Although the magnitude of the jump depends on the sharpness of the transition, the relative change in the jump is independent of the transition width provided that two samples have the same transition width. This is the case for the two isotope samples, as seen from the magnetization curves shown in Fig. 10. One can see that the ferromagnetic transition of the samples is very sharp, and that the transition widths of the two isotope samples are the same, i.e., the two curves are the same but for a parallel shift. Therefore, the

two isotope samples have the same transition width, which ensures that the observed large isotope effect on  $\Delta\beta(T_C)$  is intrinsic.

The asymmetric peak in the thermal-expansion coefficient observed for these samples and no hysteresis in  $\beta(T)$  within the accuracy of our measurements ( $\sim 0.1$  K) may indicate a second-order ferromagnetic transition. For a second-order phase transition, there is a thermodynamic relation

$$d \ln T_C / dP = 3\Delta\beta(T_C) / \Delta C_P(T_C), \quad (4)$$

where  $C_P$  is the specific heat. For  $\text{La}_{0.67}\text{Ca}_{0.33}\text{MnO}_3$ ,  $\Delta\beta(T_C) = 4.2 \times 10^{-5} \text{ K}^{-1}$  (see Fig. 9b),  $\Delta C_P = 50 \text{ J/moleK}$  [50], and unit volume =  $60 \text{ \AA}^3$ . Substituting the above values into Eq. 4, we obtain  $d \ln T_C / dP = 0.07 \text{ GPa}^{-1}$ , in excellent agreement with the measured value ( $\sim 0.06 \text{ GPa}^{-1}$  [45]). Thus the ferromagnetic transition in  $\text{La}_{0.67}\text{Ca}_{0.33}\text{MnO}_3$  seems to be of second order.

We now turn to the isotope dependence of  $\Delta\beta(T_C)$ . From Eq. 4, we see that there must be a corresponding dependence of  $d \ln T_C / dP$  on the oxygen mass  $M_O$  provided that  $\Delta C_P$  is independent of  $M_O$ . This should be the case, since  $\Delta C_P(T_C)$  arises from

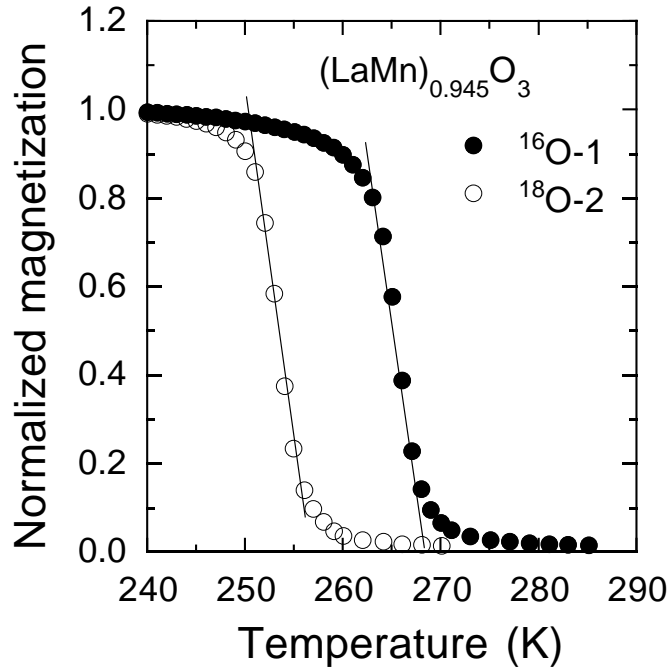


Figure 10: Temperature dependence of the low-field magnetization for the  $^{16}\text{O}$  and  $^{18}\text{O}$  samples of  $(\text{LaMn})_{0.945}\text{O}_3$ . The figure is after Ref. [22].

entropy changes due to a combination of ferromagnetic ordering of the Mn spins, and delocalization of charge carriers [50, 51], neither of which contributions should be influenced by  $M_O$ . So the oxygen isotope effect on  $\Delta\beta(T_C)$  is caused by the  $M_O$  dependence of  $d \ln T_C / dP$ . The  $M_O$  dependence of  $d \ln T_C / dP$  can be understood in terms of the empirical relation:  $d \ln T_C / dP \propto \exp(-0.016T_C)$ , as discussed above (also see Ref. [22]). This relation implies that the relative change in  $d \ln T_C / dP$  is equal to  $-0.016\Delta T_C$ . So a decrease of  $T_C$  by 12 or 10 K due to an increase of the oxygen isotope mass will lead to a relative increase of  $d \ln T_C / dP$  by 19 or 16%, which is in fair agreement with our measured value of 24(3) or 16(3)% for the relative change in  $\Delta\beta(T_C)$ . Therefore, this provides a quantitative explanation for the observed colossal oxygen-isotope effect on

$\Delta\beta(T_C)$ .

#### 4.4 Metal-Insulator Transition Induced by Oxygen Isotope Substitution.

As discussed above, the manganese-based perovskites  $\text{Ln}_{1-x}\text{A}_x\text{MnO}_3$  exhibit many remarkable features. With a decrease of temperature, a variety of phase transformations occur depending on the doping and average ionic radius  $\langle r_A \rangle$  of the cations in the  $\text{Ln}_{1-x}\text{A}_x$  site. The ferromagnetic transition temperature for the  $x = 1/3$  samples de-

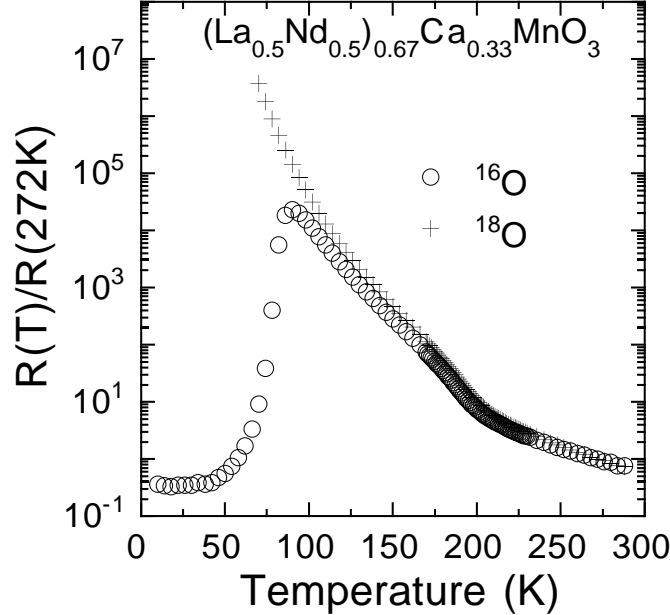


Figure 11: The temperature dependence of the resistivity (normalized to the resistivity at 272 K) for the  $^{16}\text{O}$  and  $^{18}\text{O}$  samples of  $(\text{La}_{0.5}\text{Nd}_{0.5})_{0.67}\text{Ca}_{0.33}\text{MnO}_3$ .

creases with a decrease of  $\langle r_A \rangle$ . When  $\langle r_A \rangle$  is less than a critical value, the ground state is not a metallic and ferromagnetic state, but an insulating and charge-ordered state. The compound  $(\text{La}_{0.5}\text{Nd}_{0.5})_{0.67}\text{Ca}_{0.33}\text{MnO}_3$  is just near this critical point, and shows a metallic and ferromagnetic state when the sample is prepared in  $^{16}\text{O}$  gas environment.

We have carried out the oxygen isotope substitution for this chosen compound  $(\text{La}_{0.5}\text{Nd}_{0.5})_{0.67}\text{Ca}_{0.33}\text{MnO}_3$ . We discovered [23] a novel crossover from a metallic to an insulating ground state by simply replacing the  $^{16}\text{O}$  with the  $^{18}\text{O}$  isotope. In Fig. 11, we show the temperature dependence of the zero-field resistivity (normalized to the resistivity at 272 K) for the  $^{16}\text{O}$  and  $^{18}\text{O}$  samples of  $(\text{La}_{0.5}\text{Nd}_{0.5})_{0.67}\text{Ca}_{0.33}\text{MnO}_3$ . The data were taken upon cooling down, while in Ref. [23] the data were taken upon warming up. It is surprising that the  $^{16}\text{O}$  sample shows a metallic ground state while the  $^{18}\text{O}$  sample exhibits an insulating ground state (the resistance of the  $^{18}\text{O}$  sample at 5 K is too large to measure). Somewhat later, the anomalous effect was confirmed by a Russian group [52] in the compound  $\text{La}_{0.175}\text{Pr}_{0.525}\text{Ca}_{0.3}\text{MnO}_3$ .

In the present experiment the sample quality is important because the resistivity of a polycrystalline sample depends on the grain boundaries. For a dense sample, the resistivity should be mainly contributed from the interior of the grains, and may represent an intrinsic electrical property of the material. In order to confirm that this is indeed the case, we show in Fig. 12, the dependences of the magnetization on temperature (Fig. 12a), and on magnetic field (Fig. 12b) for the two isotope samples. The temperature dependence of the magnetization was measured in a magnetic field of

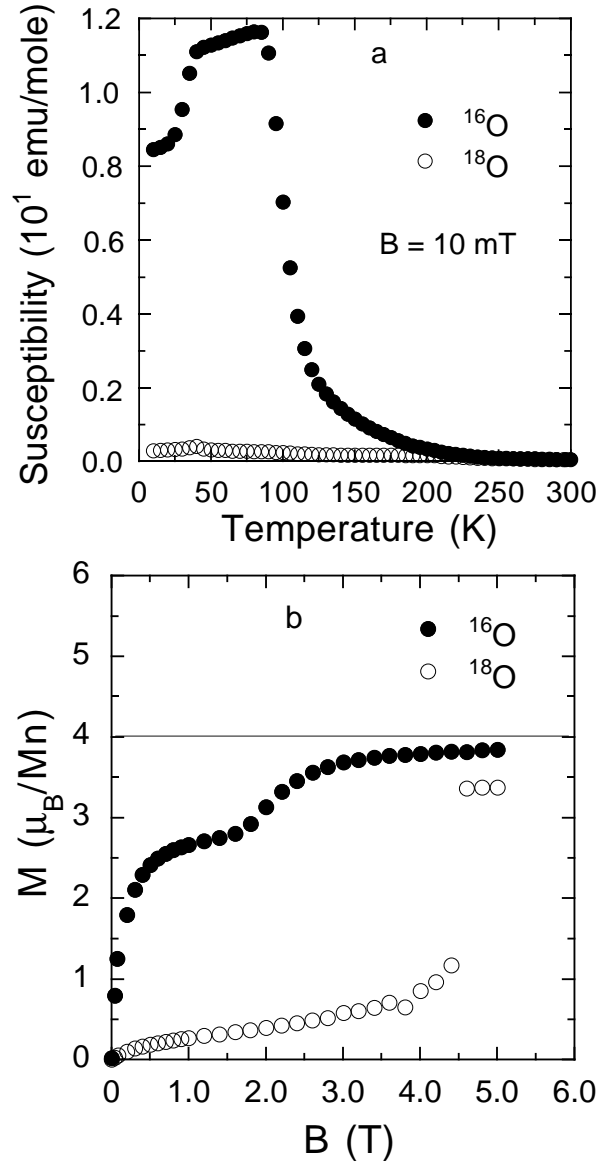


Figure 12: The dependences of the magnetization on temperature (a), and on magnetic field at 5 K (b) for the  $^{16}\text{O}$  and  $^{18}\text{O}$  samples of  $(\text{La}_{0.5}\text{Nd}_{0.5})_{0.67}\text{Ca}_{0.33}\text{MnO}_3$ . The figure is reproduced from [23].

10 mT after the samples were cooled in the field to 5 K. It is clear that the dependences of the magnetization on both temperature and magnetic field are very different for the two isotope samples. The  $^{16}\text{O}$  sample undergoes a ferromagnetic transition at about 140 K, while the  $^{18}\text{O}$  sample does not. The ferromagnetic ground state for the  $^{16}\text{O}$  sample is consistent with a metallic state at low temperatures. Another anomalous feature shown in Fig. 12b is that the  $^{18}\text{O}$  sample has a small moment below a magnetic field of about 4.5 T, then the magnetization undergoes a sudden jump towards a saturated moment. This result also implies that the ground state of the  $^{18}\text{O}$  sample is not ferromagnetic in zero field, in agreement with the resistivity data above.

So far there are no theories that can explain the novel crossover from a metallic to an insulating state by simply changing the oxygen isotope from  $^{16}\text{O}$  to  $^{18}\text{O}$ . Nevertheless, there seems to be a consensus that a strong Jahn-Teller effect in manganites leads to the formation of lattice-polarons, and that most experimental results can be explained by double-exchange and lattice-polaronic effects [30, 21]. On the basis of double-exchange

and Jahn-Teller lattice coupling to charge carriers, Millis *et al.* [21] have shown that a metal-insulator transition will occur when the electron-phonon coupling constant  $\lambda$  exceeds a critical value. The coupling constant  $\lambda$  is proportional to  $E_{JT}/\bar{t}$ , where  $E_{JT}$  is the Jahn-Teller stabilization energy,  $\bar{t}$  is the hopping integral which can be renormalized by the spin-disorder due to double-exchange. Thus this model can explain an insulator-metal transition as the temperature is reduced through  $T_C$  below which the spins become ordered, increasing  $\bar{t}$  and thereby reducing  $\lambda$ . However, this model cannot explain the crossover from the metallic to insulating ground state by changing the oxygen mass. This is because the coupling constant  $\lambda$  ( $\propto E_{JT}/\bar{t}$ ) is independent of the oxygen mass. It is worth noting that Millis *et al.* have assumed spatially homogeneous solutions in their calculation [21], which may not be true in the case of extremely strong electron-phonon interactions.

Both thermal-expansion and small-angle neutron experiments [53] show that the  $^{16}\text{O}$  sample of  $(\text{La}_{0.5}\text{Nd}_{0.5})_{0.67}\text{Ca}_{0.33}\text{MnO}_3$  undergoes a phase segregation into insulating antiferromagnetic domains and metallic ferromagnetic domains at low temperatures. However, the  $^{18}\text{O}$  sample has a negligibly small fraction of ferromagnetic domains. Therefore, it is likely that the  $^{16}\text{O}$  sample has more mobile carriers (presumably polaronic carriers which are responsible for the ferromagnetic exchange) than the  $^{18}\text{O}$  sample. Recently, Zhou *et al.*, have indeed shown that the  $^{16}\text{O}$  sample has more mobile carriers than the  $^{18}\text{O}$  sample when  $T_C$  is low [43]. This is quite reasonable because heavier carriers (e.g., in samples with a heavier isotope mass) are more easily localized by impurity potentials. Thus, this scenario appears to be able to explain this novel isotope effect.

**4.5 Oxygen Isotope Shift of the Charge-Ordering Transition.** The real-space ordering of charge carriers in crystals is one of the most interesting phenomena in condensed matter physics. Such a charge-ordering state has been observed mostly in transition-metal based oxides, such as  $\text{Ti}_4\text{O}_7$  (Ref. [54]),  $\text{La}_{2-x}\text{Sr}_x\text{NiO}_4$  (Ref. [55]),  $(\text{La,Pr,Nd})_{0.5}\text{Ca}_{0.5}\text{MnO}_3$  (Ref. [56, 58]),  $(\text{Pr,Nd})_{0.5}\text{Sr}_{0.5}\text{MnO}_3$  (Ref. [59, 60]), etc. In particular, the charge-ordering in manganites is rather exotic. As an example, the charge-ordering state in the manganites  $\text{Nd}_{0.5}\text{Sr}_{0.5}\text{MnO}_3$  and  $\text{Pr}_{0.5}\text{Sr}_{0.5}\text{MnO}_3$  can be destroyed by a small magnetic field ( $< 10$  Tesla) [59, 60]. This implies that the charge-ordering state in these systems is not so stable, which appears to be in contradiction with a large energy gap observed from both photoemission [61] and tunneling [62] experiments. Theoretically, it has been proposed that the long-range Coulomb repulsive interaction among conduction carriers might be responsible for the charge-ordering in these systems [63, 64, 65].

Our isotope experiments do not support these theoretical models. There is a large oxygen isotope effect on the charge-ordering transition temperature in  $\text{Nd}_{0.5}\text{Sr}_{0.5}\text{MnO}_3$  and  $\text{La}_{0.5}\text{Ca}_{0.5}\text{MnO}_3$  systems [57]. In Fig. 13, we show the temperature dependence of the normalized magnetizations for the  $^{16}\text{O}$  and  $^{18}\text{O}$  samples under a magnetic field of 1 mT (Fig. 13a), and 2.5 T (Fig. 13b). The normalized magnetization is defined as  $(M(T)-M_L)/(M_H-M_L)$ , where  $M_L$  and  $M_H$  are the magnetizations at the lowest and highest temperatures shown in Fig. 13, respectively. With this normalization procedure, the curves for the  $^{16}\text{O}$  and  $^{18}\text{O}$  samples are parallel shifted. The transition from a high magnetization to a low magnetization state is a signature of the transition from a ferromagnetic to a charge-ordering (CO) state [59, 60]. Here we define the mid-point temperature on the transition curve as the charge-ordering temperature ( $T_{CO}$ ). With this definition, we find that the charge-ordering temperature for the  $^{18}\text{O}$  sample is higher than for the  $^{16}\text{O}$  sample by 21 K under  $H = 1$  mT, by 28 K under  $H = 2.5$  T, and 43

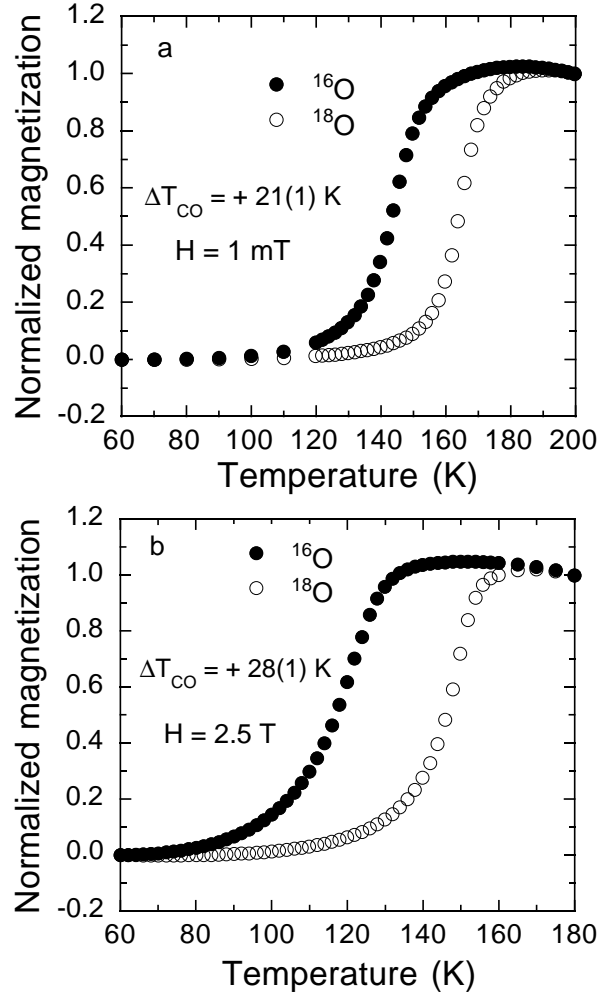


Figure 13: Oxygen isotope effect on the charge-ordering temperature of  $\text{Nd}_{0.5}\text{Sr}_{0.5}\text{MnO}_3$ : Temperature dependence of the normalized magnetization for the  $^{16}\text{O}$  and  $^{18}\text{O}$  samples under magnetic fields of 1 mT (a); 2.5 T (b).

K under  $H = 5.4$  T. This is the first observation of a colossal negative oxygen isotope shift of the charge-ordering temperature.

To show that the observed oxygen isotope shifts are intrinsic, we have performed isotope back-exchange experiments ( $^{16}\text{O} \rightarrow ^{18}\text{O}$ ;  $^{18}\text{O} \rightarrow ^{16}\text{O}$ ). In Fig. 14, we show the normalized magnetization for the  $^{16}\text{O}$  and  $^{18}\text{O}$  samples before and after isotope back-exchange. The symbol ( $\times$ ) denotes the  $^{16}\text{O}$  sample which has been back-exchanged from the original  $^{18}\text{O}$  sample (denoted by open square). The symbol (+) represents the  $^{18}\text{O}$  sample which has been back-exchanged from the original  $^{16}\text{O}$  sample (denoted by open circle). It is evident that the  $T_{CO}$  of the  $^{16}\text{O}$  ( $^{18}\text{O}$ ) sample goes back completely to that of the original  $^{18}\text{O}$  ( $^{16}\text{O}$ ) sample after the isotope back-exchange. This clearly indicates that the shift of  $T_{CO}$  is caused only by changing the oxygen isotope mass.

In Fig. 15, we show the charge-ordering temperatures of the  $^{16}\text{O}$  and  $^{18}\text{O}$  samples of  $\text{Nd}_{0.5}\text{Sr}_{0.5}\text{MnO}_3$  as a function of the external magnetic field. It is clear that, with an increase of the external magnetic field, the charge-ordering temperatures of both  $^{16}\text{O}$  and  $^{18}\text{O}$  samples decrease, but the decreasing rate for the  $^{18}\text{O}$  sample is much slower than for the  $^{16}\text{O}$  sample. This leads to an dramatic increase in the oxygen isotope shift with increasing magnetic field.

The observed large oxygen isotope shift of the charge-ordering temperature and its strong dependence on applied magnetic field are difficult to understand on the basis

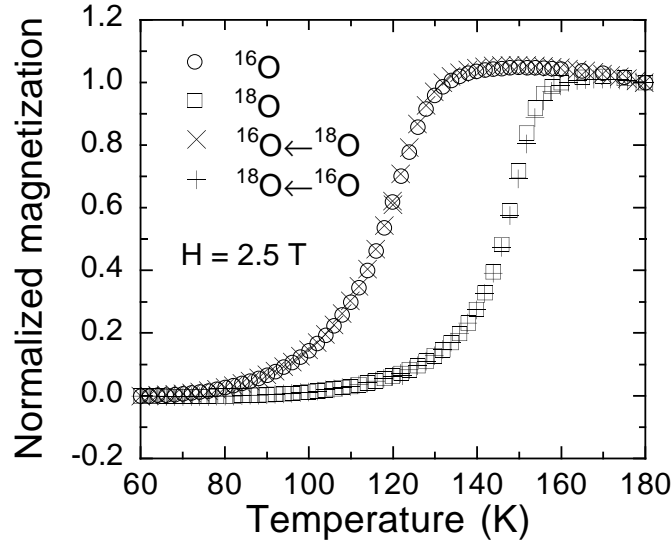


Figure 14: Oxygen isotope back-exchange result for  $\text{Nd}_{0.5}\text{Sr}_{0.5}\text{MnO}_3$ .

of the existing theories. In most theoretical models, the charge-ordering arises from a long-range Coulomb repulsive interaction between carriers [63, 64, 65]. So these models predict no isotope effect, and cannot explain our present results.

If the charge-ordering in the manganites is related to small polaron ordering, one may be able to explain the oxygen isotope shift of the charge-ordering temperature in zero magnetic field. This is because the effective mass of polaronic carriers is larger

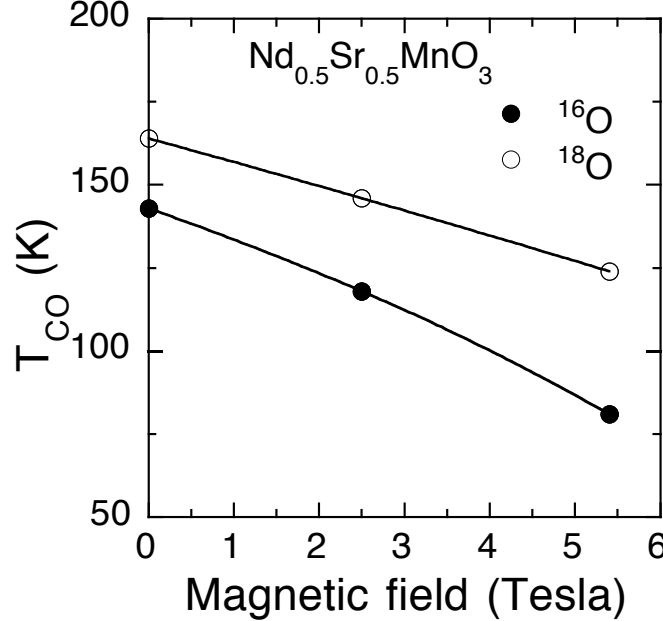


Figure 15: Magnetic field dependence of the charge-ordering temperatures of the  $^{16}\text{O}$  and  $^{18}\text{O}$  samples of  $\text{Nd}_{0.5}\text{Sr}_{0.5}\text{MnO}_3$ .

for a heavier isotope mass, and the larger the carrier mass, the more stable the charge-ordering state. As a result, one would expect a higher  $T_{CO}$  in samples with a heavier isotope mass. Thus this model can qualitatively explain the observed isotope effect in zero magnetic field. However, it cannot explain why a small magnetic field ( $< 10$  Tesla corresponding to an energy of about 10 K) can destroy the charge-ordering state

in  $\text{Nd}_{0.5}\text{Sr}_{0.5}\text{MnO}_3$  where a large energy gap ( $> 1000$  K) was observed [61, 62]. The observed large energy gap implies that the charge-ordering state, if it is a polaronic ordering state, must be stable and cannot be destroyed by a small magnetic field.

Now we consider a theory of bipolaronic charge ordering [66, 12]. On the basis of this theory [66, 12], the bipolaron charge ordering temperature is a function of both the repulsive interaction  $v$  among bipolarons and the bipolaron hopping integral  $t^*$ ,

$$T_{CO} \propto zv\sqrt{1 - (t^*/v)^2} \sqrt{1 + (1 - 2n)^2 - \frac{2(1 - 2n)}{\sqrt{1 - (t^*/v)^2}}}, \quad (5)$$

where  $z$  is the number of the nearest neighbour ions,  $n$  is the average number of bipolarons per unit cell.

In the present case,  $z = 6$  and  $n = 0.25$ , so

$$T_{CO} \propto 6v\sqrt{1 - (t^*/v)^2} \sqrt{1.25 - 1/\sqrt{1 - (t^*/v)^2}}. \quad (6)$$

Since  $t^*$  could strongly depend on the isotope mass, one might expect a large oxygen isotope effect on the charge-ordering temperature as  $t^*/v$  is close to 0.6 (when seen from Eq. 6). A small magnetic field could melt the bipolaron ordered state by reducing the density of the bipolaronic carriers. This is because the charge-ordering temperature is very sensitive to  $n$  when  $t^*/v$  is close to 0.6 and  $n$  is near 0.25 (see Eq. 5). Meanwhile there is no difficulty in explaining the observed large energy gap which can be related to the binding energy of the bipolarons.

## 5 CONCLUDING REMARKS

We have observed various oxygen isotope effects in doped manganite systems. Our results clearly indicate that lattice vibrations play an essential role in various magnetic and electrical properties of manganites. The observed colossal oxygen isotope effect on the charge-ordering temperature, and the unusual temperature dependence of the EPR linewidth suggest that bipolaronic charge carriers may exist in these compounds. This is consistent with other experiments such as tunneling [49], photoemission [29], high-resolution electron diffraction [67], and optical measurements [68]. It is likely that the charge carriers in manganites are heavy onsite bipolarons [67]. This is in contrast with the intersite bipolarons in cuprates, which is not heavy according to a model [12], and recent experiments [8]. Any viable theory which is proposed to describe the physics of manganites must be able to explain all the isotope effects observed.

**ACKNOWLEDGEMENT:** We would like to thank A. S. Alexandrov, and A. J. Millis for useful discussions. The work is partially supported by the Swiss National Science Foundation and NSF of the United States.

## References

- [1] M. K. Crawford, M. N. Kunchur, W. E. Farneth, E. M. McCarron III, and S. J. Poon, Phys. Rev. B **41**, 282 (1990)
- [2] J. P. Franck, S. Harker and J. H. Brewer, Phys. Rev. Lett. **71**, 283 (1993)
- [3] H. J. Bornemann, and D. E. Morris, Phys. Rev. B **44**, 5322 (1991)

- [4] G. M. Zhao, M. B. Hunt, H. Keller, and K. A. Müller, *Nature (London)* **385**, 236 (1997)
- [5] G. M. Zhao and D. E. Morris, *Phys. Rev. B* **51**, 16487 (1995)
- [6] G. M. Zhao, K. K. Sinha, A. P. B. Sinha, and D. E. Morris, *Phys. Rev. B* **52**, 6840 (1995)
- [7] G. M. Zhao, J. W. Ager III, and D. E. Morris, *Phys. Rev. B* **54**, 14982 (1996)
- [8] G. M. Zhao, K. Conder, H. Keller, and K. A. Müller, *J. Phys.:Condens. Matter* (in press)
- [9] G. M. Zhao, V. Kirtikar, K. K. Singh, A. P. B. Sinha, and D. E. Morris, *Phys. Rev. B* **54**, 14956 (1996)
- [10] D. Zech, H. Keller, K. Conder, E. Kaldis, E. Liarokapis, N. Poulakis, and K. A. Müller, *Nature (London)* **371**, 681 (1994)
- [11] D. Zech, K. Conder, H. Keller, E. Kaldis, and K. A. Müller, *Physica B* **219-220**, 136 (1996)
- [12] A. S. Alexandrov and N. F. Mott, *Polarons and bipolarons* (World Scientific, Singapore, 1995)
- [13] G. M. Zhao, K. Conder, H. Keller, and K. A. Müller, *Nature* **381**, 676 (1996)
- [14] E. O. Wollan, and W. C. Koeler, *Phys. Rev.* **100**, 545 (1955)
- [15] G. H. Jonker and J. H. van Santen, *Physica* **16**, 337 (1950)
- [16] S. Jin, T. H. Tiefel, M. McCormack, R. A. Fastnacht, R. Ramesh, and L. H. Chen, *Science* **264**, 413 (1994)
- [17] R. von Helmolt, J. Wecker, B. Holzapfel, L. Schltz, and K. Samwer, *Phys. Rev. Lett.* **71**, 2331 (1993)
- [18] C. Zener, *Phys. Rev.* **82**, 403 (1951)
- [19] P. W. Anderson and H. Hasegawa, *Phys. Rev.* **100**, 675 (1955)
- [20] A. J. Millis, P. B. Littlewood, and B. I. Shraiman, *Phys. Rev. Lett.* **74**, 5144 (1995).
- [21] A. J. Millis, B. I. Shraiman, and R. Müller, *Phys. Rev. Lett.* **77**, 175 (1996)
- [22] G. M. Zhao, M. B. Hunt and H. Keller, *Phys. Rev. Lett.* **78**, 955 (1997)
- [23] G. M. Zhao, H. Keller, J. Hofer, A. Shengelaya, and K. A. Müller, *Solid State Commun.*, **104**, 57 (1997)
- [24] M. Jaime, M. B. Salamon, M. Rubinstein, R. E. Treece, J. S. Horwitz, and D. B. Chrisey, *Phys. Rev. B* **54**, 11914 (1996)
- [25] S. J. L. Billinge, R. G. DiFrancesco, G. H. Kwei, J. J. Neumeier, and J. D. Thompson, *Phys. Rev. Lett.* **77**, 715 (1996)

- [26] J. M. De Teresa, M. R. Ibarra, P. A. Algarabel, C. Ritter, C. Marquina, J. Blasco, J. Garcia, A. del Moral, and Z. Arnold, *Nature (London)*, **386**, 256 (1997)
- [27] Y. Okimoto, T. Katsufuji, T. Ishikawa, A. Urushibara, T. Arima, and Y. Tokura, *Phys. Rev. Lett.* **75**, 109 (1995)
- [28] H. L. Ju, H.-C. Sohn, and K. M. Krishnan, *Phys. Rev. Lett.* **79**, 3230 (1997)
- [29] D. S. Dessau, T. Saitoh, C.-H. Park, Z.-X. Shen, P. Villella, N. Hamada, Y. Moritomo, and Y. Tokura, Preprint (1998)
- [30] H. Röder, J. Zang, and A. R. Bishop, *Phys. Rev. Lett.* **76**, 1356 (1996)
- [31] T. Saitoh, A. E. Bocquet, T. Mizokawa, H. Namatame, A. Fujimori, M. Abbate, Y. Takeda, and M. Takano, *Phys. Rev. B* **51**, 13942 (1995)
- [32] T. Holstein, *Ann. Phys. (N. Y.)*, **8**, 325 (1959)
- [33] D. Emin and T. Holstein, *Ann. Phys. (N. Y.)*, **53**, 439 (1969)
- [34] K.-H. Höck, H. Nickisch, and H. Thomas, *Helv. Phys. Acta.* **56**, 237 (1983)
- [35] H. Kamimura, *Int. J. Mod. Phys. B* **1**, 873 (1987)
- [36] P. W. Anderson, *Phys. Rev. Lett.* **34**, 953 (1975)
- [37] R. A. Street and N. F. Mott, *Phys. Rev. Lett.* **35**, 1293 (1975)
- [38] S. Lakkis, C. Schlenker, B. K. Chakraverty, R. Buder, and M. Marezio, *Phys. Rev. B* **14**, 1429 (1976)
- [39] K. A. Müller, G. M. Zhao, K. Conder, and H. Keller, *J. Phys.:Condens. Matter* **10**, L291 (1998)
- [40] G. M. Zhao and D. E. Morris, 1995 (unpublished)
- [41] Y. Moritomo, A. Asamitsu, and Y. Tokura, *Phys. Rev. B* **51**, 16491 (1995)
- [42] G. M. Zhao, K. Ghosh, and R. L. Greene, 1998 (to be published)
- [43] J.-S. Zhou and J. B. Goodenough, *Phys. Rev. Lett.* **80**, 2665 (1998)
- [44] J.-S. Zhou, W. Archibald, and J. B. Goodenough, *Nature (London)* **381**, 770 (1996)
- [45] J. J. Neumeier, M. F. Hundley, J. D. Thompson, and R. H. Heffner, *Phys. Rev. B* **52**, R7006 (1995)
- [46] J. P. Franck, I. Isaac, W. Chen, J. Chrzanowski, and J. C. Irwin, Preprint (1998)
- [47] A. Shengelaya, G. M. Zhao, H. Keller, and K. A. Müller, *Phys. Rev. Lett.* **77**, 5296 (1996).
- [48] S. E. Lofland, P. Kim, P. Dahiroc, S. M. Bhagat, S. D. Tyagi, S. G. Karabashev, D. A. Shulyatev, A. A. Arsenov, and Y. Mukovskii, *Phys. Lett. A* **233**, 476 (1997)
- [49] A. Biswas, S. Elizabeth, A. K. Raychaudhuri, and H. L. Bhat, cond-matt/9806084

- [50] A. P. Ramirez, P. Schiffer, S-W. Cheong, C. H. Chen, W. Bao, T. T. M. Palstra, P. L. Gammel, D. J. Bishop, and B. Zegarski, *Phys. Rev. Lett.* **76**, 3188 (1996)
- [51] J. M. D. Coey, M. Viret, L. Ranno, and K. Ounadjela, *Phys. Rev. Lett.* **75**, 3910 (1995)
- [52] N. A. Babushkina, L. M. Belova, O. Yu. Gorbenko, A. R. Kaul, A. A. Bosak, V. I. Ozhigin and K. I. Kugel, *Nature (London)* **391**, 159 (1998)
- [53] M. R. Ibarra, G. M. Zhao, J. M. De Teresa, B. Garcia-Landa, Z. Arnold, C. Marquina, P. A. Algarabel, and H. Keller, *Phys. Rev. B* **57**, 7446 (1998)
- [54] M. Marezio, D. B. Mcwhan, P. D. Dernier, and J. P. Remeika, *Phys. Rev. Lett.* **28**, 1390 (1972)
- [55] C. H. Chen, S.-W. Cheong, and A. S. Cooper, *Phys. Rev. Lett.* **71**, 2461 (1993)
- [56] C. H. Chen, and S.-W. Cheong, *Phys. Rev. Lett.* **76**, 4042 (1996)
- [57] G. M. Zhao, K. Ghosh, H. Keller, and R. L. Greene, 1998 (to be published)
- [58] M. Tokunaga, N. Miura, Y. Tomioka, and Y. Tokura, *Phys. Rev. B* **57**, 5259 (1998)
- [59] H. Kuwahara, Y. Tomioka, A. Asamitsu, Y. Moritomo, and Y. Tokura, *Science* **270**, 961 (1995)
- [60] Y. Tomioka, A. Asamitsu, Y. Moritomo, H. Kuwahara, and Y. Tokura, *Phys. Rev. Lett.* **74**, 5108 (1995)
- [61] A. Chainani, H. Kumigashira, T. Takahashi, Y. Tomioka, H. Kuwahara, and Y. Tokura, *Phys. Rev. B* **56**, R15513 (1997)
- [62] A. Biswas, A. K. Raychaudhuri, R. Mahendiran, A. Guha, R. Mahesh, and C. N. R. Rao, *J. Phys.:Condens. Matter* **9**, L355 (1997)
- [63] V. I. Anisimov, I. S. Elfimov, M. A. Korotin, and K. Terakura, *Phys. Rev. B* **55**, 15494 (1997)
- [64] S. K. Mishra, R. Pandit, and S. Satpathy, *Phys. Rev. B* **56**, 2316 (1997)
- [65] L. Sheng and C. S. Ting, *Phys. Rev. B* **57**, 5265 (1997)
- [66] A. S. Alexandrov and J. Ranninger, *Phys. Rev. B* **23**, 1796 (1981)
- [67] W. Bao, S. A. Carter, C. H. Chen, S.-W. Cheong, B. Batlogg, and Z. Fisk, *Solid State Commun.* **98**, 55 (1996)
- [68] P. Calvani, P. Dore, S. Lupi, A. Paolone, P. Maselli, P. Giura, B. Ruzicka, S.-W. Cheong, and W. Sadowski, *J. Supercond.* **10**, 293 (1997)